


Unexpected paths to cooperation on tied hyperbolic networks

MAJA DUH^{1,4}, MARKO GOSAK^{1,2,4} and MATJAŽ PERC^{1,3,4,5,6(a)} 

¹ Faculty of Natural Sciences and Mathematics, University of Maribor - Koroska cesta 160, 2000 Maribor, Slovenia

² Faculty of Medicine, University of Maribor - Taborska ulica 8, 2000 Maribor, Slovenia

³ Department of Medical Research, China Medical University Hospital, China Medical University - Taichung, Taiwan

⁴ Alma Mater Europaea - Slovenska ulica 17, 2000 Maribor, Slovenia

⁵ Complexity Science Hub Vienna - Josefstadtterstrasse 39, 1080 Vienna, Austria

⁶ Department of Physics, Kyung Hee University - 26 Kyungheedae-ro, Dongdaemun-gu, Seoul, Republic of Korea

received 23 May 2023; accepted in final form 7 June 2023

published online 23 June 2023

Abstract – Hyperbolic networks have high clustering, short average path lengths, and community structure, which are all properties that are commonly associated with social networks. As such, these networks constitute the perfect playing ground for probing factors that may affect public cooperation in realistic scenarios. And although much is already known about the evolution of cooperation on networks, we here consider the public goods game on tied hyperbolic networks, such that payoffs in one network layer influence the payoffs in the other and vice versa. We also consider random, assortative, and disassortative mixing in the networks to account for varying connections between players over time. While our research confirms the overall positive impact of interdependent payoffs, we also find that mixing on the network where cooperation thrives may strongly promote the cooperation in the other network, while destroying it completely in the former. We show that this is related to the mapping of lower payoffs from one network to the other, where cooperators in one network benefit from the failure of cooperators in the other network. Namely, as soon as the multiplication factor for the public goods is high enough to nullify the negative effects of mixing and cooperators thus recover, the positive effect on cooperation in the other network vanishes. We determine optimal conditions for this phenomenon in terms of the frequency of mixing and the strength of ties between the payoffs on both networks, and we discuss the implications of our research for enhanced cooperation in coupled populations, in particular in the light of mutual success not always being desirable for cooperation to thrive.

Copyright © 2023 EPLA

Introduction. – The emergence and survival of cooperative behaviour among selfish individuals is one of the major challenges that continues to captivate the interest of scientists across various disciplines [1]. The use of evolutionary game theory has emerged as a key tool in this effort, offering a robust theoretical framework for describing the evolutionary dynamics of strategies in social dilemmas [2–4]. On the other hand, the advances made in network science greatly enhance our understanding of many complex systems in the real world, including the evolution of cooperation in social dilemmas [5–7]. By representing individuals as nodes in a network, and their social interactions as links between nodes, researchers can analyse the structure and dynamics of social networks to gain insights into the mechanisms that promote cooperation and develop strategies for fostering it

in real-world settings. Over the past two decades, research has demonstrated that the structure of social networks is a critical factor in determining the prevalence of cooperation [8–11]. The shift from regular grids and lattices to complex social networks has proven as a crucial step forward in creating more realistic network models. Such models include various types of interactions, such as scale-free [12–20], small-world [21–25], random [26], hierarchical [27–29] and coevolving networks [30–33]. Lately, new network models have emerged that effectively capture the most important structural properties of real-world networks, such as random geometric graphs in hyperbolic spaces. These models are known for having realistic features, such as small diameter, high clustering, community structure, and a heterogeneous degree distribution [34,35], making them a popular choice for simulating a range of social phenomena, including evolutionary game theory [36–41].

^(a)E-mail: mat.jaz.perc@gmail.com (corresponding author)

Meanwhile, there has been a shift in focus from single and isolated networks to multilayer and interdependent networks [42–52]. This is due to the fact that individuals often belong to multiple networks simultaneously, making interdependent networks more relevant for describing real-world systems than isolated networks. In one of the seminal works, Buldyrev *et al.* [53] investigated a cascade of failure on the interdependent networks and found that seemingly irrelevant changes in one network can have catastrophic consequence in another network. Along this way, Wang *et al.* used the concept of interdependent networks to study the evolution of public cooperation [42]. They introduced the interdependence through the utility function and showed that the bias in the utility function can effectively influence the level of public cooperation. Since then, numerous mechanisms have been proposed to explore the cooperative behaviour on interdependent networks, including individual popularity [54], heterogeneous coupling between lattices [50], information sharing [55,56], self-organization [52,57], migration and stochastic imitation [48], assortative and disassortative matching between layers [58] as well as third party interventions [59]. Noteworthy, it has also been shown that network reciprocity affects cooperative behavior in multilayer networks only under weak coupling, whereas for strong coupling, the effect of network reciprocity disappears [47].

In real-life situations, individuals often move around, leading to changes in their network of interactions. Mobility is a crucial characteristic of social and biological systems, and it plays an important role in the study of evolutionary games. To understand the impact of mobility on the evolution of cooperation, researchers have proposed different mobility models [48,60–65]. The movements of individuals can either be independent of the evolutionary dynamics [66–69], or driven by the evolutionary dynamics, where players move based on their payoff [32,70,71], success [72] or aspiration [73,74]. Additionally, numerous studies have examined the mixing of players in relation to node degrees. These studies have demonstrated that various types of migrations can have different impacts on the evolution of cooperation in heterogeneous networks [40,75]. The concept of degree mixing has also been applied to multilayer networks. For instance, Wang *et al.* [61] studied the impact of assortative and disassortative mixing on two-layer scale-free networks and concluded, that degree mixing in multilayer networks hinders the evolution of cooperation.

In this paper we further explore the principles of public cooperation in the context of multi-layered interactions by means of public goods game on tied hyperbolic networks, so that players across the two network layers are connected through the utility function, which couples the payoffs across both layers. We additionally incorporate in our model different types of mixing protocols (random, assortative and disassortative), where mixing of players can be performed on one (A or B) or both (A and B) layers. In our simulations we then focus on how the interplay

between different types of player migrations and interlayer interactions affects the evolution of public cooperation.

Mathematical model. – We studied the public goods game on two interconnected network layers, A and B, with each node within the layer being occupied by one player. We use random geometric graphs in hyperbolic spaces to simulate the structure of interactions between players in each layer. To create the network, we began with $n = 2$ connected nodes and then introduced new nodes (i) that were mapped onto a hyperbolic disc using polar coordinates that were randomly assigned: $\theta_i = 2\pi u_1$ and $r_i = \frac{1}{\beta} \cos^{-1} [1 + \cosh(\beta R_{hd} - 1)u_2]$, where $R_{hd} = 1$ reflects the radius of the hyperbolic disc, $\beta = 0.1$ is the internal growth parameter, and u_1 and u_2 are independent random variables sampled from the uniform distribution on a unit interval. Each new i -th node connects with n existing nodes with a probability that is proportional to the distance between the i -th and the j -th node: $d_{ij} = \cosh^{-1}[\cosh(r_i) \cosh(r_j) - \sinh(r_i) \sinh(r_j) \cos(\Delta\theta_{ij})]$, where $\Delta\theta_{ij} = \pi - |\pi - |\theta_i - \theta_j||$ denotes the angular distance [35]. This leads to a broad-scale network with an average degree 4 [40]. Building upon the idea of multilayer network concepts, players do not only interact with their neighbours within the same layer, but also with players in the other network layer. The interdependence between the layers was established through utility functions that were guided by the interlayer connections. The latter were established so that each player in layer A gets connected with one player in layer B with the shortest possible connection. A schematic presentation of the multilayer network model is shown in fig. 1(a).

The resulting networks are utilized in the classical public goods game, where individual players are represented by nodes, and the interactive relationships between them are characterized by the edges. Each player i has k_i direct neighbours in the same network layer (*i.e.*, the degree of the individual player) and one i' indirect partner in the other network layer. Initially, each player is randomly assigned as a cooperator (C) or defector (D) with an equal probability. Players accumulate their payoffs on both network layers following the same procedure. Namely, each player participates in $g = k_i + 1$ overlapping groups, where cooperators contribute a fixed cost to the public good ($s_i = 1$) while defectors contribute nothing ($s_i = 0$). Afterwards, the overall contributions are multiplied by the synergy factor $R > 1$, and the resulting amount is then redistributed equally among all players in the group. Accordingly, the payoff of a player in each group g obtained on the network layer A is P_i and $P_{i'}$ on layer B, while the overall payoff received in all the groups is the sum $P_i = \sum_g P_i^g$ and $P_{i'} = \sum_g P_{i'}^g$. As the number of direct neighbours varies between individuals, the synergy factor R is normalized with the size of the corresponding group to ensure a meaningful comparison of the results [76].

As noted previously, there exist so-called dependency links between both network layers A and B, where each

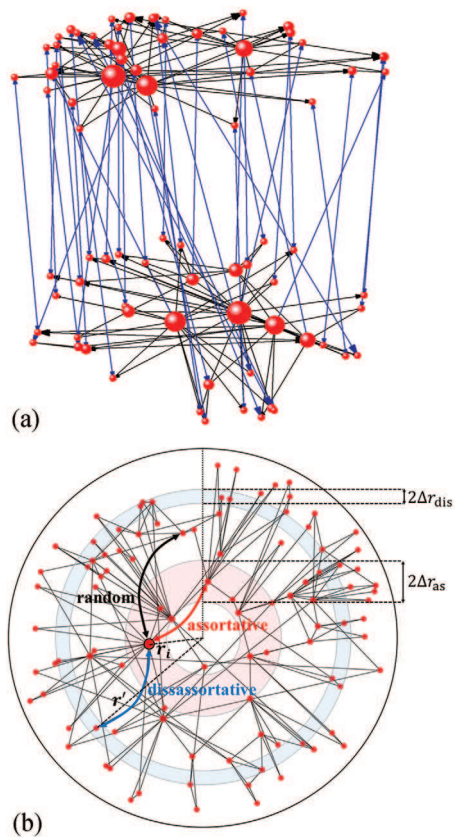


Fig. 1: Graphical presentation of the multilayer public goods game model with mixing of the players. (a) A scheme of the two-layer network where the interactions between players within each layer (black lines) are modelled by the geometric model in hyperbolic spaces. Blue lines indicate the interlayer connections between the two layers, which were established so that the distance between the connected players in different layers was minimal. Only 40 nodes per network layer are displayed here for illustrative purposes. (b) Schematic representation of the three different types of mixing. The i -th player at the radial position r_i exchanges positions with the j -th player, whose position is determined arbitrary in case of random mixing (black arrow), within an annulus centered at the mean radius r_i with width $2\Delta r_{as}$ in the scenario of assortative mixing (red arrow), within an annulus centered at the mean radius r' with width $2\Delta r_{dis}$ when considering disassortative mixing (blue arrow). Only 100 nodes within the network layer are shown for illustration purposes, although in our simulations we used $N = 2500$ nodes per network layer.

player i in the network layer A has exactly one external partner i' in the network layer B, and the same applies in reverse. To take into account that the payoff of a player depends also on the state of a player in another layer, the interlayer connections can be expressed as the utility functions

$$U_i = \alpha P_i + (1 - \alpha) P_{i'}, \quad U_{i'} = (1 - \alpha) P_{i'} + \alpha P_i. \quad (1)$$

α determines the strength of external links or the bias between the payoffs of player i and i' on the two network

layers, with $\alpha = 0$ ($\alpha = 1$) indicating that the utility primarily relies on the payoff of player i' (player i) as in the single network scenario [40]. When α is between 0 and 0.5, player i is primarily affected by the payoff of its external partner i' . For $\alpha = 0.5$ both payoffs are taken into consideration equally strongly by both players i and i' . Conversely, when α is between 0.5 and 1, the roles of players i and i' are reversed, resulting in fully symmetric outcomes [42]. Henceforth, network layer A is considered as the primary network, and the values of α are restricted to the range of $[0, 0.5]$ for the subsequent explanations.

We simulate the evolutionary process in accordance with the standard Monte Carlo simulation. After randomly selecting one player i , one of its neighbors j on the layer A, and the corresponding external partners i' and j' on layer B, the corresponding payoffs and utility functions can be calculated. Considering that strategy transfers are allowed from neighbors on a given network layer only, player i adopts the strategy of player j with a probability determined by the Fermi function

$$W(s_i \rightarrow s_j) = \frac{1}{1 + \exp[(U_j - U_i)/K]}, \quad (2)$$

where K denotes uncertainty related to the strategy adoption process and is set to 0.5 without loss of generality [77]. The adoption of a strategy by player i' from player j' occurs in a similar manner with the use of their respective utilities $U_{i'}$ and $U_{j'}$ in eq. (2).

To introduce mixing of players, we implemented a mixing process after every m -th Monte Carlo step. During a mixing step, each player had a chance to exchange their site with another randomly selected player on the same network layer, on average once. In most of our calculations the mixing frequency was set to $m = 10$, unless stated otherwise. This means that randomly selected pairs were switched after every 10th Monte Carlo step. We considered different types of mixing protocols: i) random mixing, where places of players were exchanged irrespective of their positions; ii) assortative mixing, where players with similar distances from the center of the hyperbolic disc were swapped; iii) disassortative mixing, where players close to the center were replaced by remote players and vice versa. With this, we took into account that the degree of a node tends to increase as it gets closer to the center, and that nodes farther away from the center have lower degrees and are considered peripheral nodes.

How different types of mixing are incorporated in our model is illustrated in fig. 1(b). In principle, in either scenario a randomly selected i -th player located at a radial distance r_i exchanges the place with the randomly selected j -th player. The latter is chosen arbitrary in case of random mixing (black arrow). When considering assortative mixing, the j -th player is selected from the nodes located within an annulus centered at the mean radius r_i , with a width of $2\Delta r_{as}$ (red arrow), whilst in the case of disassortative mixing, it is selected from the annulus at the mean radius r' , with a width of $2\Delta r_{dis}$ (blue arrow).

The widths of both annuli, $2\Delta r_{as}$ and $2\Delta r_{dis}$, denote the locations of 5% of nodes with the closest radial distances to the nodes located at radius r_i or r' . Moreover, in the scenario of disassortative mixing, the radius r' defines the radial distance to the j -th player, whose relative distance rank is $R(j) = 1 - R(i)$, with $R(i)$ denoting the relative distance-based rank of the selected i -th player located at the radial distance r_i .

In our calculations we considered $N = 2500$ players in each network layer. To determine the equilibrium fraction of cooperators, we averaged the last 10000 generations after a transient period of 100000 Monte Carlo time steps. Additionally, the final results were averaged over 400 independent runs for each set of parameter values (20 different initial conditions and 20 different network realizations).

Results. – We start by presenting the influence of the payoff bias α and additional random mixing of players on the evolution of cooperation on two interdependent random hyperbolic networks. Figure 2 shows the fraction of cooperators f_C on both network layers as a function of the normalized synergy factor R/G . Panels on the left side of fig. 2 display the results for layer A, while panels on the right side show the results for layer B. Three mixing options are considered: mixing only on layer A, mixing only on layer B, and mixing on both layers A and B. Random mixing is applied after every 10th full Monte Carlo step, where N randomly selected pairs exchange places. We first focus on the results of the game without mixing (solid grey lines with circles). The results clearly show that the evolution of public cooperation on both network layers depends significantly on the value of the bias α , *i.e.*, the stronger the bias, the higher the level of public cooperation. When α is set to 0.01 (fig. 2(a) and (b)), the evolution on layer A is mainly (99%) influenced by the payoffs of players in layer B, while the evolution on layer B is almost identical with the evolution on a single random hyperbolic network [40]. Cooperators on layer B dominate completely for approximately $R/G > 0.6$, while layer A is occupied by both cooperators and defectors for the whole range of R/G . For $\alpha = 0.2$ (fig. 2(c) and (d)), the success level of cooperators on layer A is slightly higher, while at B the results are similar to those obtained for $\alpha = 0.01$. According to eq. (1), at $\alpha = 0.49$ (fig. 2(e) and (f)) the difference between the two networks vanishes completely, as both payoffs (P_i and $P_{i'}$) play the same role in evaluating utility.

Introducing random mixing of players only on layer A (solid dark blue lines with rectangles) has no impact on the evolution of cooperation on layer B when α is set to 0.01 (fig. 2(b)). This is understandable, since the game on B is almost not influenced by the payoffs of players in layer A. However, mixing on layer A shifts the critical value of the normalized synergy factor, above which cooperators emerge, to higher R/G values and increases the success level of cooperators on layer A (fig. 2(a)). This effect is even more significant for $\alpha = 0.2$ (fig. 2(c) and (d)),

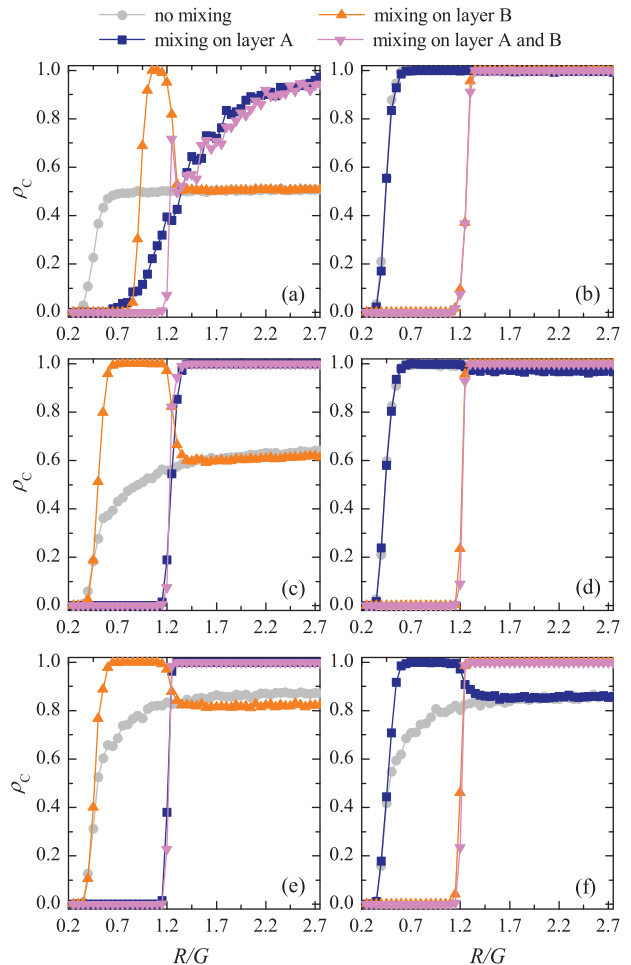


Fig. 2: While the evolution of public cooperation on two interdependent network layers depends significantly on the value of the bias α , additional mixing of players in the networks leads to very unexpected results. Depicted is the fraction of cooperators f_C as a function of the normalized synergy factor R/G , as obtained on two interdependent random hyperbolic graphs for $\alpha = 0.01$ (a) and (b), $\alpha = 0.2$ (c) and (d), and $\alpha = 0.49$ (e) and (f). The left three panels (a), (c) and (e) show results for the layer A, while the right three panels (b), (d) and (f) show results for the layer B. In all panels results for random mixing on one (A or B) layer and both (A and B) layers are presented. The solid grey line with circles shows the corresponding result for the public goods game on two interdependent random hyperbolic graphs without mixing. The size of each network layer is $N = 2500$, and the mixing frequency is set to $m = 10$.

where transformations begin to emerge on layer B as well. These changes become most pronounced when α equals 0.49 (fig. 2(e) and (f)), where interesting phenomena occur, which will be further addressed in continuation. Furthermore, when random mixing of players is introduced only on layer B (solid orange lines with triangles), the outcomes are even more surprising. Results presented in the top two panels ($\alpha = 0.01$) evidence that mixing on layer B impairs the evolutionary success of cooperators on this layer, while promote it for certain values of the normalised synergy factor R/G on layer A. This range of R/G

values, where mixing on layer B improves cooperation on layer A, is even wider for $\alpha = 0.2$ (fig. 2(c)), while cooperation on layer B is still suppressed (fig. 2(d)). When $\alpha = 0.49$ (the bottom two panels of fig. 2), mixing on layer B (A) evidently promotes cooperation on the other layer —layer A (B)— while on the same layer (where mixing is performed) the critical value of the normalized synergy factor, above which cooperators emerge, shifts to higher R/G values (~ 1.15). When the normalized multiplication factor is high enough, cooperators dominate completely, which cannot be achieved without the introduction of mixing on this layer. Finally, mixing on both layers A and B (solid pink lines with inverted triangles) produces on layer A almost identical outcomes as mixing only on layer A. Similarly, the results of mixing on both layers for layer B are nearly identical to those obtained with mixing only on layer B. Moreover, this is true for all investigated α values.

Next, we investigated the effect of different types of mixing protocols (random, assortative, and disassortative) on the evolution of cooperation on two interdependent networks, with the focus on mixing on layer B only. Figure 3 depicts the fraction of cooperators as a function of the normalized multiplication factor R/G , as obtained for different combinations of the payoff bias α and different mixing protocols. The left and right panels in fig. 3 show the results for layers A and B, respectively. To provide a point of reference, we display the outcomes of the game without mixing (indicated by a solid grey line with circles) in all panels for comparison. The differences between different mixing types are clearly visible for $\alpha = 0.01$ (fig. 3(a) and (b)) and $\alpha = 0.2$ (fig. 3(c) and (d)). It is evident that random mixing has the most significant impact, followed by disassortative mixing, which has a slightly lower impact, and finally, assortative mixing, which has an even smaller impact. For $\alpha = 0.49$ (fig. 3(e) and (f)), assortative and disassortative mixing hardly evoke a visible difference in the fraction of cooperators compared with the case, where random mixing is applied. Comparing different types of mixing with the case where no mixing is introduced, we observe that assortative and disassortative mixing have a very similar effect on the evolutionary success of cooperators as random mixing, for all selected α values. Regardless of the type of mixing, mixing on the network layer where primary (without mixing) cooperation is successful (in our case, layer B) can greatly enhance cooperation in the other network layer (in our case, layer A), but it may lead to its total breakdown in the former. However, once the synergy factor becomes large enough, cooperators on the primary network layer recover and the positive effect on cooperation in the other layer disappears. We conclude that the transfer of lower payoffs from one network layer to another plays a crucial role in this phenomenon, as it allows cooperators in one layer to take advantage of the failure of cooperators in the other layer.

To gain a better understanding of this phenomenon, we limit our focus solely to the random mixing type, where mixing is performed only on layer B, and vary the mixing

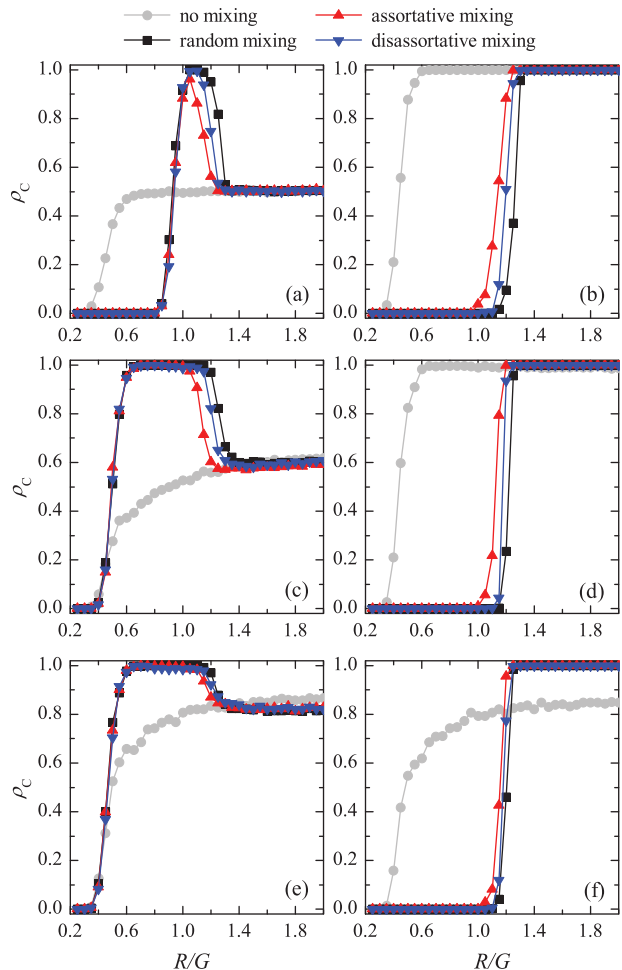


Fig. 3: Mixing on the network layer where cooperation is successful can strongly encourage cooperation in another network layer, while completely destroying it in the first, regardless of the type of mixing. All six panels present the fraction of cooperators f_C as a function of the normalized multiplication factor R/G , as obtained on two interdependent random hyperbolic graphs A (left three panels) and B (right three panels) for three different values of the bias α : $\alpha = 0.01$ (a) and (b), $\alpha = 0.2$ (c) and (d), and $\alpha = 0.49$ (e) and (f). In all panels results for three mixing types (random, assortative and disassortative mixing), where mixing is performed only on layer B, are presented. The solid grey line with circles shows the corresponding result for the public goods game on two interdependent random hyperbolic graphs without mixing. The size of each network layer is $N = 2500$, and the mixing frequency is $m = 10$.

frequency m . Figure 4 depicts the fraction of cooperators f_C as a function of the normalized synergy factor R/G for $\alpha = 0.01$ (fig. 4(a)), $\alpha = 0.2$ (fig. 4(b)) and $\alpha = 0.49$ (fig. 4(c)). To facilitate comparison, results for both layers (A and B) are presented in the same panel. The results confer that mixing on layer B impairs the evolutionary success of cooperators on the same layer —layer B (indicated by solid lines with open rectangles)— while enhances cooperation in the other network layer —layer A

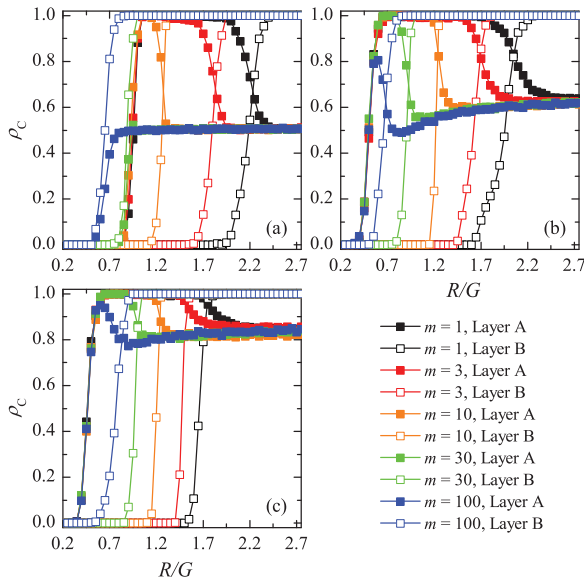


Fig. 4: Once the multiplication factor becomes high enough to cancel out the negative effects of mixing in one network layer (in our case layer B), then the positive effect on cooperation in the other network layer (in our case layer A) disappears. Depicted is the fraction of cooperators f_C as a function of the normalized synergy factor R/G , as obtained on two interdependent random hyperbolic graphs A (closed rectangles) and B (open rectangles) for $\alpha = 0.01$ (a), $\alpha = 0.2$ (b) and $\alpha = 0.49$ (c). In all panels results for random mixing on layer B for five different mixing frequencies m are presented. The size of each network layer is $N = 2500$.

(indicated by solid lines with closed rectangles)— and the more so the smaller the value of m . When the synergy factor reaches a certain threshold, the beneficial impact of cooperation in layer A diminishes and cooperators in layer B experience a recovery in their success level. The effect can be observed for all selected values of the mixing frequency m when α is set to 0.2 and 0.49. However, when $\alpha = 0.01$ and the mixing frequency is 100, the critical value of the normalized synergy factor R/G , required for cooperators to emerge, only shifts slightly to higher values in both layers.

Discussion. — Over the last two decades, researchers have utilized network science to identify the most suitable network topologies that accurately depict real-world networks and help understand collective social behaviour. Recently, multilayer networks have gained much attention in this respect, not only because they offer a solid framework to describe diverse types of genuine interactions but also because the combination of different network topologies across various layers can affect the evolution of cooperation in nontrivial ways [43,78,79]. In a recent study by Wu *et al.* [49], the evolution of cooperation was investigated in a multigame model composed of the Prisoner’s Dilemma and Snowdrift game on interdependent networks with different topologies. Specifically, interdependent net-

works formed by two square lattices were found to promote the evolution of cooperation, while coupling between two scale-free networks was shown to inhibit cooperation. To investigate further the role of interlayer interactions in heterogeneous networks, we studied here the multiplayer public goods game on two interdependent random geometric graphs in hyperbolic spaces, where the interdependence between both layers is introduced by means of the utility function [42]. Our findings suggest that introducing biased considerations of payoffs can be beneficial for promoting public cooperation. Similar results have been obtained on two interdependent scale-free networks [58].

Furthermore, to account for the possibility of players migrations, we studied the effect of random, assortative and disassortative mixing on one or both layers, where N selected pairs (on the same network layer) switched after each m -th Monte Carlo step. We demonstrated that such varying connections between players over time led to very unexpected outcomes. Mixing on the network layer, where cooperation is primary successful (in our case layer B), impairs the evolutionary success of cooperators on the same network layer, regardless of the type of the mixing protocol. Furthermore, the smaller the value of the mixing frequency m , the more detrimental mixing is for cooperation. This is in agreement with previous results on isolated networks [40,80]. Interestingly, our results show that cooperation can be strongly promoted in the other network layer (in our case layer A), but only for certain values of the normalized synergy factor R/G . Once the multiplication factor for the public goods reaches a certain threshold that counteracts the negative effects of mixing on the former layer, cooperators are able to recover and the positive impact on cooperation in the other layer disappears. This phenomenon can be attributed to the transfer of lower payoffs from one network layer to another, which leads to the cooperators in one layer benefiting from the failures of cooperators in the other layer.

Our aspiration is for this work to contribute to the better understanding of the evolution of public cooperation within the context of migration and multi-layered interactions, as well as to the better understanding of other forms of moral behavior by means of mathematical and agent-based modeling [81]. Furthermore, we hope to inspire other researchers to explore the utilization of tied hyperbolic networks and the various applications of agents’ mixing and mobility in similar lines of research.

This research was supported by the Slovenian Research Agency (Javna agencija za raziskovalno dejavnost RS) (Grant Nos. P1-0403, J1-2457 and J3-3077).

Data availability statement: No new data were created or analysed in this study.

REFERENCES

- [1] NOWAK M. A., *Evolutionary Dynamics* (Harvard University Press, Cambridge, Mass.) 2006.
- [2] MAYNARD SMITH J., *Evolution and the Theory of Games* (Cambridge University Press, Cambridge, UK) 1982.
- [3] SIGMUND K., *The Calculus of Selfishness* (Princeton University Press, Princeton, N.J.) 2010.
- [4] JAVARONE M. A., *Statistical Physics and Computational Methods for Evolutionary Game Theory* (Springer, New York) 2018.
- [5] BOCCALETTI S. *et al.*, *Phys. Rep.*, **424** (2006) 175.
- [6] ALBERT R. and BARABÁSI A.-L., *Rev. Mod. Phys.*, **74** (2002) 47.
- [7] ESTRADA E., *The Structure of Complex Networks: Theory and Applications* (Oxford University Press, Oxford) 2012.
- [8] NOWAK M. A., *Science*, **314** (2006) 1560.
- [9] PERC M. and SZOLNOKI A., *BioSystems*, **99** (2010) 109.
- [10] CAPRARO V. *et al.*, *Phys. Rev. E*, **101** (2020) 032305.
- [11] VILONE D. *et al.*, *J. Phys. Commun.*, **2** (2018) 025019.
- [12] SANTOS F. C. and PACHECO J. M., *Phys. Rev. Lett.*, **95** (2005) 098104.
- [13] PONCELA J. *et al.*, *New J. Phys.*, **9** (2007) 184.
- [14] MASUDA N., *Proc. R. Soc. B*, **274** (2007) 1815.
- [15] ASSENZA S. *et al.*, *Phys. Rev. E*, **78** (2008) 017101.
- [16] TANIMOTO J. *et al.*, *Phys. Rev. E*, **85** (2012) 032101.
- [17] MAO Y. *et al.*, *EPL*, **122** (2018) 50005.
- [18] CIMPEANU T. *et al.*, *Chaos, Solitons Fractals*, **167** (2023) 113051.
- [19] CIMPEANU T. *et al.*, to be published in *Dyn. Games Appl.* (2023), <https://doi.org/10.1007/s13235-023-00502-1>.
- [20] CIMPEANU T. *et al.*, *Sci. Rep.*, **12** (2022) 1723.
- [21] KIM B. J. *et al.*, *Phys. Rev. E*, **66** (2002) 021907.
- [22] MASUDA N. and AIHARA K., *Phys. Lett. A*, **313** (2003) 55.
- [23] SANTOS F. C. *et al.*, *Phys. Rev. E*, **72** (2005) 056128.
- [24] FU F. *et al.*, *Eur. Phys. J. B*, **56** (2007) 367.
- [25] LIN Z. *et al.*, *Physica A*, **553** (2020) 124665.
- [26] KUMAR A. *et al.*, *J. R. Soc. Interface*, **17** (2020) 20200491.
- [27] VUKOV J. and SZABÓ G., *Phys. Rev. E*, **71** (2005) 036133.
- [28] LEE S. *et al.*, *Phys. Rev. Lett.*, **106** (2011) 028702.
- [29] HUANG F. *et al.*, *J. Theor. Biol.*, **449** (2018) 60.
- [30] PACHECO J. M. *et al.*, *Phys. Rev. Lett.*, **97** (2006) 258103.
- [31] FU F. *et al.*, *Phys. Rev. E*, **79** (2009) 036101.
- [32] WANG C. *et al.*, *Chaos, Solitons Fractals*, **162** (2022) 112461.
- [33] CIMPEANU T. *et al.*, *Co-evolution of Social and Non-social Guilt in Structured Populations*, in *Proceedings of the 2023 International Conference on Autonomous Agents and Multiagent Systems (AAMAS '23)* (ACM) 2023, pp. 2739–2741; arXiv:2302.09859 [cs.MA] (2023).
- [34] BOGUÑA M. *et al.*, *Nat. Commun.*, **1** (2010) 62.
- [35] ZUEV K. *et al.*, *Sci. Rep.*, **5** (2015) 9421.
- [36] KLEINEBERG K.-K., *Nat. Commun.*, **8** (2017) 1888.
- [37] AMATO R. *et al.*, *Sci. Rep.*, **7** (2017) 7087.
- [38] PU J. *et al.*, *Chaos, Solitons Fractals*, **125** (2019) 146.
- [39] GOSAK M. *et al.*, *Sci. Rep.*, **11** (2021) 3093.
- [40] DUH M. *et al.*, *Chaos, Solitons Fractals*, **144** (2021) 110720.
- [41] JAVARONE M. A. and ARMANO G., *J. Phys. A: Math. Theor.*, **46** (2013) 455102.
- [42] WANG Z. *et al.*, *EPL*, **97** (2012) 48001.
- [43] WANG Z. *et al.*, *Eur. Phys. J. B*, **88** (2015) 124.
- [44] GÓMEZ-GARDEÑES J. *et al.*, *Phys. Rev. E*, **86** (2012) 056113.
- [45] BATTISTON F. *et al.*, *New J. Phys.*, **19** (2017) 073017.
- [46] SHI L. *et al.*, *Nonlinear Dyn.*, **96** (2019) 49.
- [47] LI G. and SUN X., *Physica A*, **578** (2021) 126110.
- [48] CHOWDHURY S. N. *et al.*, *Entropy*, **22** (2020) 485.
- [49] WU Y. *et al.*, *Physica D*, **447** (2023) 133692.
- [50] XIA C.-Y. *et al.*, *PLoS ONE*, **10** (2015) e0129542.
- [51] DENG Z.-H. *et al.*, *Physica A*, **510** (2018) 83.
- [52] CHU C. *et al.*, *Chaos*, **29** (2019) 013139.
- [53] BULDYREV S. V. *et al.*, *Nature*, **464** (2010) 1025.
- [54] LIU C. *et al.*, *New J. Phys.*, **20** (2018) 123012.
- [55] SZOLNOKI A. and PERC M., *New J. Phys.*, **15** (2013) 053010.
- [56] LIU J. *et al.*, *Appl. Math. Comput.*, **340** (2019) 234.
- [57] LUO C. and ZHANG X., *Commun. Nonlinear Sci. Numer. Simul.*, **42** (2017) 73.
- [58] DUH M. *et al.*, *New J. Phys.*, **21** (2019) 123016.
- [59] SONG Z. *et al.*, *Appl. Math. Comput.*, **403** (2021) 126178.
- [60] PERC M. *et al.*, *J. R. Soc. Interface*, **10** (2013) 20120997.
- [61] WANG Z. *et al.*, *Phys. Rev. E*, **89** (2014) 052813.
- [62] ZHANG S. X. L. *et al.*, *Eur. Phys. J. B*, **95** (2022) 67.
- [63] CONG R. *et al.*, *PLoS ONE*, **7** (2012) e35776.
- [64] DHAKAL S. *et al.*, *R. Soc. Open Sci.*, **9** (2022) 212000.
- [65] ARMANO G. and JAVARONE M. A., *Sci. Rep.*, **7** (2017) 1781.
- [66] CARDILLO A. *et al.*, *Phys. Rev. E*, **85** (2012) 067101.
- [67] JAVARONE M. A., *Eur. Phys. J. B*, **89** (2016) 42.
- [68] VAINSTEIN M. H. *et al.*, *J. Theor. Biol.*, **244** (2007) 722.
- [69] SICARDI E. A. *et al.*, *J. Theor. Biol.*, **256** (2009) 240.
- [70] CHEN Y.-S. *et al.*, *Physica A*, **450** (2016) 506.
- [71] HE Z. *et al.*, *Chaos, Solitons Fractals*, **141** (2020) 110421.
- [72] HELBING D. and YU W., *Proc. Natl. Acad. Sci. U.S.A.*, **106** (2009) 3680.
- [73] LIN Y.-T. *et al.*, *Physica A*, **390** (2011) 77.
- [74] WU T. *et al.*, *Phys. Rev. E*, **85** (2012) 066104.
- [75] RONG Z. *et al.*, *Phys. Rev. E*, **76** (2007) 027101.
- [76] SANTOS F. C. *et al.*, *Nature*, **454** (2008) 213.
- [77] PERC M. *et al.*, *Phys. Rep.*, **687** (2017) 1.
- [78] JUSUP M. *et al.*, *Phys. Rep.*, **948** (2022) 1.
- [79] ALVAREZ-RODRIGUEZ U. *et al.*, *Nat. Hum. Behav.*, **5** (2021) 586.
- [80] DUH M. *et al.*, *Phys. Rev. E*, **102** (2020) 032310.
- [81] CAPRARO V. and PERC M., *J. R. Soc. Interface*, **18** (2021) 20200880.